

## MICELLAR SOLUBILIZATION OF BIOPOLYMERS IN HYDROCARBON SOLVENTS. I. A STRUCTURAL MODEL FOR PROTEIN-CONTAINING REVERSE MICELLES

FRANCIS J. BONNER, ROMAIN WOLF, and PIER LUIGI LUISI<sup>1</sup>

*Technisch-Chemisches Laboratorium der ETH-Zürich  
ETH-Zentrum, 8031-Zürich, Switzerland*

Accepted July 9, 1980

Three proteins (horse liver alcohol dehydrogenase, ribonuclease, lysozyme) were solubilized in hydrocarbon with the help of reverse micelles formed by aqueous di(2-ethyl-hexyl) sodium sulfosuccinate (AOT). Sedimentation and diffusion coefficients of the micellar aggregates were measured with an analytical ultracentrifuge. Partial specific volumes were also evaluated from density measurements. The molecular weight of the protein-containing reverse micelles ( $M_r$ ) could thus be determined for each protein system at various  $w_0$  values ( $w_0 = [\text{H}_2\text{O}]/[\text{AOT}]$ ). For horse liver alcohol dehydrogenase at  $w_0 = 46.4$ , for example,  $M_r$  is ca. 2,670,000 Daltons; for lysozyme at  $w_0 = 22.5$ ,  $M_r$  is ca. 323,000 Daltons and increases by increasing  $w_0$ . On the basis of these experimentally determined molecular weights, a structural model for the protein-containing reverse micelle is proposed. The model is based upon the assumption that the protein is confined in the water pool of a spherical micelle, and that the inner core volume is the sum of the protein volume and the volume of all water molecules present in a micelle. It is possible then to calculate the micellar structure at each  $w_0$  value. For example, in the case of ribonuclease at  $w_0 = 20$ , the inner core radius is ca. 37.5 Å, and a layer of water of ca. 22 Å separates the protein surface from the surfactant layer. The possible implications of this model for the reactivity of enzymes solubilized in hydrocarbons by reverse micelles are discussed.

### INTRODUCTION

Certain surfactants, when dissolved in apolar solvents, tend to form aggregates, viz. the so-called reverse micelles, in which the polar heads of the surfactant molecules are confined in the internal core (1-3). Reverse micelles have also found interest in connection with biological systems. For example, Wells and collaborators (4-6) have described a system in which phospholipase was solubilized in diethylether/methanol by using reverse micelles of phosphatidylcholine. The study of such a system is still being actively pursued (7,8). Quite recently, this approach has been broadened and new aspects have been introduced to include various surfactants and

<sup>1</sup> Author to whom correspondence should be addressed.

hydrophylic enzymes solubilized in different hydrocarbon solvents. The groups of Martinek et al. (9), Menger and Yamada (10), Dozou et al. (11), and our own (12–14) have described these reverse micellar systems in a series of preliminary papers.

There are several possible lines of inquiry in the study of enzyme-containing reverse micelles. For example, one might be interested in the catalytic aspects of such systems for either fundamental studies or technical applications, or in the structure-stability relationship of such aggregates, or in the mass-transport phenomena of the various components of the aggregate. Finally, protein-containing micelles can be interesting as models for biological systems, as already exemplified by the work on phospholipase (4–8) and by some other recent studies, which suggest that reverse micelles can be one of the mechanisms by which certain membranes assemble *in vivo* (15).

In the present work, we address the question of structure. We develop a model for protein-containing reverse micelles based on centrifugal measurements of sedimentation and diffusion coefficients as well as experimentally determined partial specific volumes. This is done for ribonuclease (RNase) and for horse liver alcohol dehydrogenase (LADH) in the system sodium di(2-ethyl-hexyl) sulfosuccinate (AOT)–water–isooctane, as well as for lysozyme in AOT–water–*n*-octane. This model, which pictures the protein residing in a pool of water inside a more or less spherical micelle, should be considered only a first approximation. It involves a number of assumptions that will be subjected to further investigation. We show, however, that such a model appears reasonable in terms of material balances, molecular weights, sizes of equivalent spheres, and, as will be shown in the sequel to this paper, also in terms of spectroscopic properties and enzymatic activity.

#### MATERIALS AND METHODS

The enzymes horse liver alcohol dehydrogenase (LADH), and ribonuclease were obtained from Boehringer, and lysozyme was obtained from Fluka. Water solutions of LADH were obtained and assayed as described previously (30), and solutions of the other two enzymes were prepared by dissolving the enzyme powder into buffer. Concentrations were calculated on the basis of literature extinction coefficients, i.e.,  $35,300 \text{ M}^{-1} \text{ cm}^{-1}$  for LADH (16),  $9700 \text{ M}^{-1} \text{ cm}^{-1}$  for ribonuclease (17), and  $37,900 \text{ M}^{-1} \text{ cm}^{-1}$  for lysozyme (18). Isooctane puriss. was purchased from Fluka, and *n*-octane purum (Fluka) was distilled over  $\text{P}_2\text{O}_5$ . AOT was obtained from Serva and purified as described in the literature (19). Despite repeated

purification steps, UV-absorbing impurities were still present in our final preparations. Typically, a 50 mM AOT solution in hydrocarbon had an absorbance of 0.02 at 280 nm. The enzyme micellar solutions were prepared by injecting (with a microsyringe) a buffered stock solution of the enzyme into the hydrocarbon-AOT solution, and shaking mildly. Depending upon conditions (water content, protein concentration, and temperature), cloudy solutions were obtained. Only clear solutions (no scattering at 300 nm) were used for the studies reported in this work. The concentration of the enzyme solutions used for ultracentrifugation studies was in the range 3–15  $\mu$ M. The viscosity of isooctane (0.4478 cp) was taken from Zulauf and Eicke (26), and the value for *n*-octane (0.482 cp) is an interpolation of several temperature values from the literature (27).

Ultracentrifugational analyses were made in a Beckman Model E analytical ultracentrifuge, using the standard UV-monochromator, optical scanner, rotors, and cells. Well-established procedures (20) were used to determine the sedimentation coefficient, *s*, the diffusion coefficient, *D*, and then the molecular weight, *M*, from the Svedberg equation,

$$M = \frac{RT}{1 - \bar{v}\rho} \cdot \frac{s}{D} \quad (1)$$

where *R*, *T*,  $\bar{v}$ , and  $\rho$  are, respectively, the universal gas constant, absolute temperature, partial specific volume, and density of solution.

Apparent partial specific volumes were determined from very precise density measurements, i.e., to within several parts in a million, by temperature control to within  $\pm 0.02^\circ\text{C}$ , at  $30.0^\circ\text{C}$ , with a vibrating tube device (Anton Paar, Graz, Austria, Density Meter DMA-02D), and the relation (21)

$$\bar{v} = \frac{1}{x} \left[ \frac{1}{\rho} - \frac{(1-x)}{\rho_0} \right] \quad (2)$$

where *x*,  $\rho$ , and  $\rho_0$  are, respectively, the weight fraction of sedimenting entity, the density of solution, and the density of solvent. The weight fraction of sedimenting entity for this purpose was assumed to be the total weight fraction of surfactant plus water plus protein.

Velocity ultracentrifugations were made at 40,000 rpm and  $30.0^\circ\text{C}$ . The sedimentation coefficient was then determined from the slope of a plot of  $\ln r$  versus *t* based on the defining relation:

$$s = \frac{1}{w^2} \cdot \frac{d \ln r}{dt} \quad (3)$$

where *w*, *t*, and *r* are, respectively, the rotational speed, time, and radial

position of the midpoint in the optical density curve (ca. 280 nm) representing the sedimenting boundary.

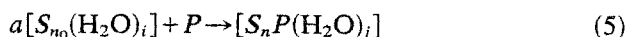
Diffusion measurements were made at 30.0°C between 1000 and 6000 rpm. Initially, sharp boundaries were formed between solvent and solution in a capillary type double-chambered cell. Diffusion coefficients were determined from the slopes of plots of  $\Delta r^2$  versus  $t$  based on the relation

$$D = \frac{1}{3.64} \cdot \frac{\Delta r^2}{t} \quad (4)$$

where  $t$  is time and  $\Delta r$  is the difference in radial position between the one-fourth and the three-fourths concentration levels in the spreading boundary, registered by optical density at 280 nm.

#### *A Structural Model and Descriptive Relations*

When a protein enters the inner core of a reverse micelle, a reorganization of the micelle probably takes place. With the assumption of one protein guest molecule per host micelle, this could be formulated as



where  $n_0$  and  $n$  are the aggregation numbers of the surfactant,  $S$ , in unfilled and filled micelles, respectively;  $i$  is the number of water molecules in the inner core of the micelle before entry of the protein molecule,  $P$ ; and  $j$  is the corresponding number of water molecules after entry. The coefficient  $a$  represents the number of "unfilled" micelles necessary to build up a filled one. Since the protein causes an enlargement of the micelle, with an increase in aggregation number and water content,  $n$  and  $j$  will be greater than  $n_0$  and  $i$ , respectively. Thus the increase of molecular weight is greater than simply the additional weight of the protein and can be expressed as

$$M_T = M_P + jM_W + nM_S \quad (6)$$

where  $M_T$ ,  $M_P$ ,  $M_W$ , and  $M_S$  are, respectively, the molecular weights of total micelle, protein, water, and surfactant. In order to evaluate the micellar parameters  $n$  and  $j$ , one can proceed as follows. Assuming that the ratio of water molecules to surfactant molecules per micelle,  $w_0$ , remains the same upon entry of the protein, i.e.,

$$w_0 = \frac{i}{n_0} = \frac{j}{n} \quad (7)$$

Eq. (6) can be rewritten as

$$M_T = M_P + nw_0M_W + nM_S \quad (8)$$

or, alternatively, as

$$M_T = M_P + jM_W + \frac{j}{w_0} M_S \quad (9)$$

Since "unmicellized" surfactant and water is negligible, a value for  $w_0$  can be obtained directly from the initially measured addition of surfactant and water. We have used values for  $M_T$  determined experimentally in the present work, and established values for  $M_P$ ,  $M_W$ , and  $M_S$  in Eqs. (8) and (9) to determine the number of surfactant molecules,  $n$ , and the number of water molecules,  $j$ , per protein-containing micelle (Tables 1 and 2, see below).

In order to determine the micellar size, we now proceed as follows. Assuming the micelles to be spherical, the inner core volume  $v_{ic}$ , of the protein-containing micelles, can be expressed as

$$v_{ic} = \frac{4}{3}\pi r_0^3 = jV_W + V_P \quad (10)$$

where  $r_0$ ,  $V_W$ , and  $V_P$  are, respectively, the inner core radius, the volume occupied by water, and the volume occupied by protein. The experimental values for  $M_T$ , determined from Eq. (1), were used in Eq. (9) to determine values for  $j$ . Values for  $V_W$  and  $V_P$  were established as follows. A value of  $29.9 \text{ \AA}^3$  was used for a water molecule (22). Considering the proteins as prolate ellipsoids with the largest dimension as the major and the next largest as the minor axis, and using  $38 \times 28 \text{ \AA}$  for RNase (23),  $45 \times 30 \text{ \AA}$  for lysozyme (24),  $110 \times 60 \text{ \AA}$  for horse LADH (25), the respective volumes were determined to be  $15,600 \text{ \AA}^3$ ,  $21,200 \text{ \AA}^3$ , and  $207,400 \text{ \AA}^3$ . Equation (10) could then be solved for the corresponding inner core radius,  $r_0$ .

The inner core radius can, of course, be used to calculate a corresponding inner core surface area, viz.,

$$A_{ic} = 4\pi r_0^2 \quad (11)$$

which should have absorbed on it  $n$  surfactant molecules. The surface area per surfactant molecule can be expressed as

$$f_s = \frac{4\pi r_0^2}{n} \quad (12)$$

and for the presently used system (AOT in isooctane), the surface area is available from the literature as a function of  $w_0$  (22). Therefore, assuming that the presence of protein in the inner core does not affect this packing density, these data can be used to calculate values of  $n$  to be compared with values determined from Eq. (8). Likewise, Eqs. (10) and (12) can be

combined to give the relation

$$\frac{4}{3}\pi r_0^3 = \frac{4\pi r_0^2}{f_s} w_0 V_W + V_p \quad (13)$$

which can be used to calculate an inner core radius,  $r_0$ , from established values of  $f_s$ ,  $w_0$ ,  $V_W$ , and  $V_p$ . Moreover, the thickness of the surfactant shell can be added to give the radius,  $r_t$ , of the protein-containing micelle represented as a sphere, viz.,

$$r_t = r_0 + l_s \quad (14)$$

where the thickness of the surfactant shell,  $l_s$ , in the present system can be considered the length of one AOT molecule, taken as 12 Å (26).

A useful way to visualize the results of Eq. (13) is given in Fig. 1, which shows the dependence of the dimensions of the micelle as a function of the macroscopic parameter  $w_0$  for the case of unfilled micelles, and for the case of micelles filled with ribonuclease and horse liver alcohol dehydrogenase. For the relatively small ribonuclease molecule, the dimensions of the filled and unfilled micelles are practically the same at  $w_0$  ca. 30. At smaller  $w_0$

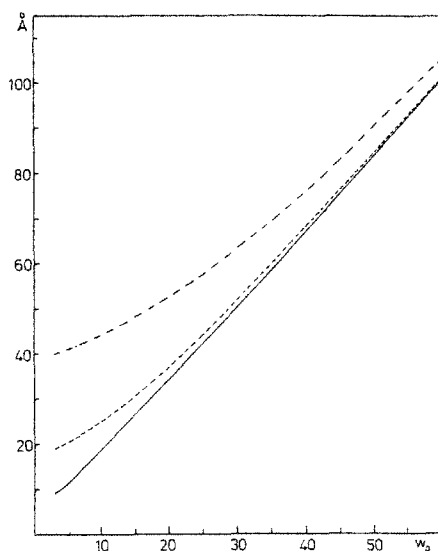


FIG. 1. Inner core radius  $r_0$  (Å) as a function of the molar ratio  $w_0 = [\text{H}_2\text{O}]/[\text{AOT}]$ , calculated from Eq. (13), for —, unfilled micelles; ---, micelles containing one RNase molecule; and - · - ·, micelles containing one LADH molecule.

values, the filled micelles are larger, and this difference is obviously much more marked in the case of horse liver alcohol dehydrogenase. For example, at  $w_0 = 15$ , the LADH-containing micelles are twice as large as the unfilled ones.

Figure 2 shows more in detail the case of ribonuclease at  $w_0 = 5$  and  $w_0 = 20$ . In the first case, a layer of water of ca.  $5 \text{ \AA}$  separates the protein from the layer of surfactant molecules; in the second case, the water layer is  $22 \text{ \AA}$ .

The radius  $r_t$  can be compared with the Stokes radius  $r_h$ , determined from the viscosity of the solvent, and the diffusion coefficient of the protein-containing micelles by means of the relation

$$r_h = \frac{kT}{6\pi\eta D} \quad (15)$$

which follows directly from combining Stokes's law

$$f = 6\pi\eta r_h \quad (16)$$

with the well-known relation

$$D = \frac{kT}{f} \quad (17)$$

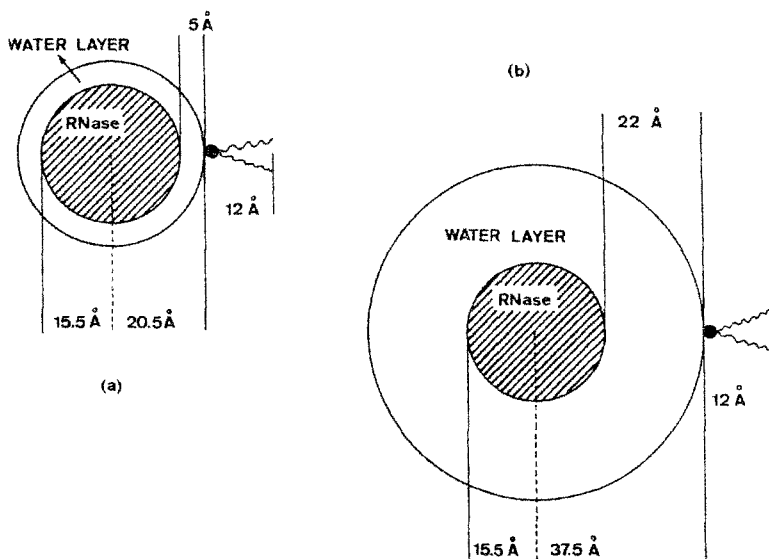


FIG. 2. Model (cross-section) and dimensions for a micelle containing one RNase molecule. (a)  $w_0 = [\text{H}_2\text{O}]/[\text{AOT}] = 5$ ; (b)  $w_0 = [\text{H}_2\text{O}]/[\text{AOT}] = 20$ .

where  $k$ ,  $T$ ,  $\eta$ ,  $D$ , and  $f$ , respectively, are the Boltzmann constant, absolute temperature, viscosity of the solvent, diffusion coefficient, and friction factor. Implicit in this approach is the assumption that the micelles can be adequately approximated by rigid and uncharged spheres moving in a continuous medium without slippage.

The fraction of material involved in the protein-containing micelles can be estimated from a straightforward material balance using (a) the equivalence in the concentration of protein and protein-containing micelles, and (b) established values of aggregation number,  $n_0$ , of surfactant for a particular  $w_0$  value.

## RESULTS AND INTERPRETATIONS

Having discussed the theoretical setup, let us consider now the experimental data, and extract from these the various structural parameters for the micellar aggregate. Table 1 gives the results of the ultracentrifugal analysis for the proteins RNase, lysozyme, and horse LADH solubilized in the system AOT-water-isooctane (or  $n$ -octane), i.e., density of solution,  $\rho$ , partial specific volume,  $\bar{v}$ , sedimentation coefficient,  $s$ , diffusion coefficient,  $D$ , and molecular weight of the protein-containing micelles,  $M_T$ , at various ratios of water molecules to surfactant molecules,  $w_0$ .

Note that, for each enzyme system, the sedimentation coefficient and the molecular weight of each protein-aggregate increase by increasing the water content. This is to be expected, since it has already been shown (22,26) that the size of reverse micelles can be increased by increasing  $w_0$ . As mentioned in the experimental part, the absorption signal of the protein was monitored in the 280 nm region, so that essentially only the protein-containing micelles are observed in the ultracentrifugation and diffusion runs. Usually, the sedimenting boundary was relatively sharp (Fig. 3), which is indicative of homogeneity. This agrees with the accepted view that the reverse micelles are rather monodisperse (but more studies are needed in order to better establish this point). Table 2 compiles the other structural parameters obtained for our model at the same composition,  $w_0$ , i.e., the number of surfactant molecules,  $n$ , and the number of water molecules,  $j$ , in each protein-containing micelle, and the inner core radius,  $r_0$ .

Note that even with the lowest  $w_0$  there are more than 500 water molecules per protein, so that the picture of a protein molecule embedded in a water pool is a reasonable one. One should, however, note that not all the water will be in a free form. In fact, one would expect a certain amount of water be bound to surfactant, protein, and buffer ions. According to NMR data (31), and other measurements (19), under conditions of excess water,



TABLE 1. Characterization of the Enzyme-Containing Micelles<sup>a</sup>

System	$w_0$	$s$ (s <sup>-1</sup> )	$D$ (cm <sup>2</sup> /s)	$\bar{v}$ (cm <sup>3</sup> /g)	$\rho$ (g/cm <sup>3</sup> )	$M_t$	$r_h$ (Å)
RNase							
Isooctane/AOT(0.05 M)	5.7	$14.4 \times 10^{-13}$	$1.5 \times 10^{-6}$	0.8979	0.6938	64,000	32.7
RNase							
Isooctane/AOT(0.05 M)	11.1	$20.3 \times 10^{-13}$	$1.0 \times 10^{-6}$	0.9086	0.6954	138,000	49.1
RNase							
Isooctane/AOT(0.05 M)	22.3	$29.2 \times 10^{-13}$	$6.0 \times 10^{-7}$	0.9280	0.6984	348,000	82.5
Lysozyme							
<i>n</i> -Octane/AOT(0.05 M)	22.5	$38.0 \times 10^{-13}$	$8.8 \times 10^{-7}$	0.9282	0.7131	323,00	52.7
Lysozyme							
<i>n</i> -Octane/AOT(0.05 M)	27.4	$57.0 \times 10^{-13}$	$7.0 \times 10^{-7}$	0.9320	0.7133	611,000	65.7
LADH							
Isooctane/AOT(0.05 M)	46.4	$95.7 \times 10^{-13}$	$2.8 \times 10^{-7}$	0.9594	0.7046	2,670,000	177.7

<sup>a</sup> For the definitions of  $w_0$ ,  $S$ ,  $D$ ,  $\bar{v}$ ,  $\rho$ ,  $M_t$ , and  $r_h$ , see Eqs. (1), (2), (6), and (15).

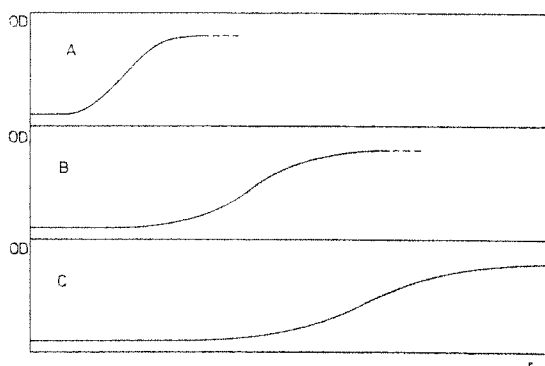


FIG. 3. Scanner traces of sedimentation profile (concentration in terms of optical density at 284 nm versus radial position) at 40,000 rpm and 30°C for the system RNase/AOT (0.05 M)/isooctane with  $w_0 = [\text{H}_2\text{O}]/[\text{AOT}] = 11.1$ ; curve A approximately 20 min after the start of sedimentation, with curves B and C at successive 16 min intervals.

AOT tends to firmly bind as many as 6–7 water molecules, but it is reasonable to assume that due to competition with the protein and the buffer ions, this will be considerably less in the protein-containing micelles at low  $w_0$  values ( $w_0 < 10$ ).

In principle, it would be possible to elaborate our model to take into account the water bound to AOT, and to discriminate among the various types of free and bound water. However, in this paper we have chosen not to

TABLE 2. Calculated Micellar Parameters<sup>a</sup>

System	$w_0$	$n$	$j$	$r_0$ (Å)
RNase				
Isooctane/AOT(0.05 M)	5.7	91	521	19.5
RNase				
Isooctane/AOT(0.05 M)	11.1	193	2128	26.6
RNase				
Isooctane/AOT(0.05 M)	22.3	395	8823	40.6
Lysozyme				
<i>n</i> -Octane/AOT(0.05 M)	22.5	364	8195	39.9
Lysozyme				
<i>n</i> -Octane/AOT(0.05 M)	27.4	636	17,452	50.6
LADH				
Isooctane/AOT(0.05 M)	46.4	2022	93,844	89.6

<sup>a</sup>For the definitions of  $w_0$ ,  $n$ ,  $j$ , and  $r_0$ , see Eqs. (5), (7), and (10). For  $M_p$  [Eqs. (6), (8) and (9)], 13,680, 14,000, and 80,000 were used for RNase, lysozyme, and LADH, respectively.

attempt this, because we believe that this complication is not needed at the present time. But these considerations do indicate the way to go for a more sophisticated model, which could be developed once corresponding experimental data at a higher degree of precision become available. At this point also, the approximation of spherical micelles could be discarded in favor of more detailed structures (e.g., ellipsoids of various types).

It is interesting to compare the Stokes radius with the total micellar radius, which is given by the sum of  $r_0$  (in Table 2) plus  $l_s$  (the linear dimension of an AOT molecule, taken as 12 Å). The agreement tends to be better at lower  $w_0$  values (see, in particular, the case of RNase). It is possible that the poor agreement obtained in some cases (for example, LADH and RNase at high  $w_0$ ) is due to deviations from sphericity of the aggregate, or to thermodynamic nonideality.

#### IMPLICATIONS OF THE MODEL AND CONCLUDING REMARKS

According to our model for micellar solubilization of proteins in organic solvents, a protein molecule is immersed in a pool of water, which is in turn encapsulated in a spherical micelle, thus preventing denaturation. The spherical shape, while a convenience for the calculations and perhaps a close approximation to reality for a number of systems and concentrations, should not, however, be taken as the general, stringent structural prerequisite. Also, we do not want to imply that the model presented here is the only possible one. One can envisage situations in which two or more protein molecules are present in the same micelle, in which the surfactants interact directly with the protein molecule, or in which the more hydrophobic parts of the protein are directly exposed to the organic solvent. While more data are needed to test if and when all these various possibilities occur, the simple model presented here may serve as a useful preliminary working hypothesis. Thus spectroscopic studies (in particular circular dichroism and fluorescence) should show whether the solubilized biopolymer experiences a water environment [this point is discussed in the following paper (32)].

There are other considerations arising from the proposed model that could be of interest. For example, one notices that at relatively large  $w_0$  values ( $w \geq 30$ ) the physicochemical properties of water in the protein-containing micelles will probably differ very little from those of bulk water. However, at lower  $w_0$  values, a large part of the water will be bound (to the protein, to the surfactant, and to other ions). One should then recognize that properties such as pH, dielectric constant, and other physicochemical properties pertaining to the protein environment may be hard to evaluate and even to define.

An important aspect that does not directly arise from simple inspection of our model is the dynamic behavior of the reverse micelles. It has been shown that a very fast exchange of material is possible among micelles (28). In particular, Eicke and coworkers (29) argued that when the reverse micelles collide, they may remain in contact for a time which is comparable with diffusion time.

Figure 4 tries to represent this situation in the case of an enzymatic reaction taking place in the micellar hydrocarbon phase, in the simple case in which the enzyme E and the substrate S are only soluble in the water pool. The active E-S is formed when a enzyme-containing micelle collides and partly "melts" with a substrate-containing micelle. After reaction, the product is eventually eliminated via an "unfilled" micelle, which collides and partly melts with the E-P-containing micelle.

Another question that should be clarified in connection with the proposed model is how to deal with the concentration of the reagents. Since reaction is localized in the water pool, one could use a "local" concentration, i.e., referred to the water pool alone. We will define such a concentration as  $c_{wp}$ . Alternatively, one might consider overall concentrations (defined as  $c_{ov}$ ), i.e., referred to the whole system, which are generally those that one measures experimentally (for example, spectrophotometrically). For a

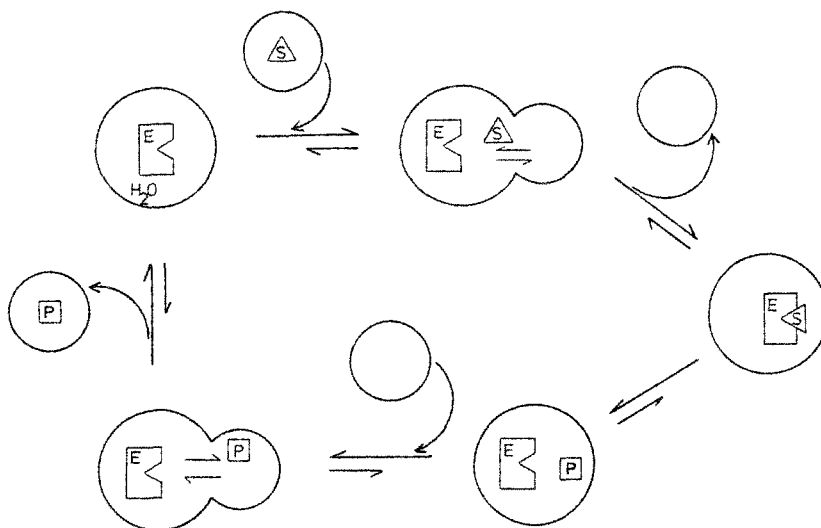


FIG. 4. Schematic representation of an enzymatic reaction in a reverse micellar system. E, S, and P represent the enzyme, the substrate, and the product, respectively. The circles represent the water pool (cross-section) of the reverse micelle. Water is present in all micelles, but is not expressly indicated for the sake of simplicity.

reagent that is only soluble in the water pool,  $c_{ov} = c_{wp} \cdot F_w$ , where  $F_w$  is the volume fraction  $F_w$  of water ( $F_w = \text{volume of water/total volume}$ ). If the reagent partitions between the water phase and the hydrocarbon phase, with concentrations  $c_{wp}$  and  $c_{hyd}$ , respectively, then

$$c_{ov} = c_{hyd}(1 - F_w) + c_{wp}F_w \quad (7)$$

or, alternatively,

$$\frac{c_{ov}}{c_{wp}} = F_w + P(1 - F_w) \quad (8)$$

where  $P$  is the partition coefficient ( $P = c_{hyd}/c_{wp}$ ). The two sets of concentrations correspond to two different ways of viewing the micellar systems. It follows that one can define two different values for the Michaelis-Menten constant, or for the dissociation constant. Notice, however, that the turnover number of an enzymatic reaction (i.e., velocity normalized for the enzyme concentration) is unaffected by the choice of the reference system. The spectrophotometrically measured  $(dp/dt)_{ov}$  is in fact an overall quantity, and could be divided by  $E_{ov}$  to give a turnover number ( $s^{-1}$ ); if the reaction is viewed in the water pool, then the turnover number is defined by  $(dp/dt)_{wp} \cdot 1/E_{wp}$ , where  $(dp/dt)_{wp} = F_w^{-1} (dp/dt)_{ov}$ , which gives the same number as in the other case.

## REFERENCES

1. FENDLER, J. H., and FENDLER, E. J. (1975) *In* Catalysis in Micellar and Macromolecular Systems, Academic, New York.
2. EICKE, H. F. (1980) *Top. Curr. Chem.* 87 : 85-145.
3. KITAHARA, A. (1980) *Adv. Colloid Interface Sci.* 12 : 109-140.
4. MISIOROWSKY, R. L., and WELLS, M. A. (1974) *Biochemistry* 13 : 4921-4927.
5. POON, P. H., and WELLS, M. A. (1974) *Biochemistry* 13 : 4928-4936.
6. WELLS, M. A. (1974) *Biochemistry* 13 : 4937-4942.
7. ALLGYER, T. T., and WELLS, M. A. (1978) *Adv. Exp. Med. Biol.* 101 : 153-163.
8. ALLGYER, T. T., and WELLS, M. A. (1979) *Biochemistry* 18 : 4364-4361.
9. MARTINEK, K., LEVASHOV, A. V., KLYACHKO, N. L., and BEREZIN, I. V. (1977) *Dokl. Akad. Nauk SSSR* 236 : 920-923.
10. MENDER, F. M., and YAMADA, K. (1979) *J. Am. Chem. Soc.* 101 : 6731-6734.
11. DOUZOU, P., KEH, E., and BALNY, C. (1979) *Proc. Natl. Acad. Sci. USA* 76 : 681-684.
12. LUISI, P. L., HENNINGER, F., JOPPICH, M., DOSSENA, A., and CASNATI, G. (1977) *Biochem. Biophys. Res. Commun.* 74 : 1384-1389.
13. LUISI, P. L., BONNER, F., PELLEGRINI, A., WIGET, P., and WOLF, R. (1979) *Helv. Chim. Acta* 62 : 740-753.
14. WOLF, R., and LUISI, P. L. (1979) *Biochem. Biophys. Res. Commun.* 89 : 209-217.
15. DE KRUIFF, B., CULLIS, P. R., and VERKLEIJ, A. J. (1980) *TIBS* (March), pp. 79-81.
16. SUND, H., and THEORELL, H. (1963) *In* The Enzymes, 2nd ed., Vol. VII, BOYER, P. D. (ed.), Academic, New York. pp. 25-57.

17. SAGE, H. J., and SINGER, S. J. (1962) *Biochem.* 1 : 305-317.
18. JOLLES, J., JAUREGULL-ADELL, J., BERNIEC, J., and JOLLES, P. (1963) *Biochim. Biophys. Acta* 78 : 668-689.
19. WONG, M., THOMAS, J. K., and GRÄTZEL, M. (1976) *J. Am. Chem. Soc.* 98 : 2391-2397.
20. CHERVENKA, C. H. (1970) *In* A Manual of Methods for the Analytical Ultracentrifuge, Spinco Division of Beckmann Instruments, Inc., Palo Alto, Calif.
21. BRANDRUP, J., and IMMERGUT, E. H. (eds.) (1975) *Polymer Handbook*, 2nd ed., Wiley, New York, IV-64.
22. EICKE, H. F., and REHAK, J. (1976) *Helv. Chim. Acta* 59 : 2883-2891.
23. KARTHA, G., BELLO, J., and HARKER, D. (1967) *Nature* 213 : 862-865.
24. IMOTO, T., JOHNSON, L. N., NORTH, A. C. T., PHILLIPS, D. C., and RUPLEY, J. A. (1972) *In* The Enzymes, 3rd ed., Vol. VII, BOYER, P. D. (ed.), Academic, New York, p. 692.
25. BRÄNDÉN, C. I., JÖRNVALL, H., EKLUND, H., and FURUGREN, B. (1975) *In* The Enzymes, 3rd ed., Vol. XI, BOYER, P. D. (ed.), Academic, New York, p. 120.
26. ZULAUF, M., and EICKE, H. F. (1979) *J. Phys. Chem.* 83 : 480-486.
27. *Handbook and Chemistry and Physics* (1979), 59th ed., CRC Press, Cleveland.
28. MENDER, F. M., DONOHUE, J. A., and WILLIAMS, R. F. (1973) *J. Am. Chem. Soc.* 95 : 286-288.
29. EICKE, H. F., SHEPHARD, J. C. W., and STEINMANN, A. (1976) *J. Colloid Interface Sci.* 56 : 168-176.
30. THEORELL, H., and YONETANI, T. (1963) *Biochem. Z.* 338 : 557-563.
31. WONG, M., THOMAS, J. K., and NOWAK, T. (1977) *J. Am. Chem. Soc.* 99 : 4730-4736.
32. MEIER, P., and LUISI, P. L. (1980) *J. Solid-Phase Biochem.* 5 : 269-282, this issue.